International Journal of Microwave and Wireless Technologies, 2013, 5(2), 115–122.
doi:10.1017/S1759078713000056

RESEARCH PAPER

Application of embedding dimension estimation to Volterra series-based behavioral modeling and predistortion of wideband RF power amplifier

BILEL FEHRI AND SLIM BOUMAIZA

This paper expounds the systematic modeling of the behavior of radio frequency (RF) power amplifiers (PAs) exhibiting nonlinear, dynamic behavior. The approach begins with an analysis of the PA output signal to deduce the minimum embedding parameters required to accurately model its response, particularly the nonlinearity order and memory effects depth. The knowledge of the RF PA is then exploited in limiting the number of kernels consequently addressing the complexity of the Volterra series which has been the key hindrance to its wider practical adoption. In the proposed Volterra series model, performance is assessed and compared to memory polynomial model and dynamic deviation reduction Volterra models when used to linearize different high-power amplifiers driven with wideband signals of bandwidth up to 40 MHz. Significant linearization performance is achieved using a reduced number of kernels.

Keywords: Power amplifiers and linearizers, Modeling, Simulation and characterizations of devices and circuits

Received 21 October 2012; Revised 3 January 2013; first published online 7 February 2013

I. INTRODUCTION

Recent advances in modulation techniques and access technologies have imposed contradictory linearity and efficiency requirements on radio frequency (RF) power amplifiers (PAs). This has triggered the development of several sophisticated linearization techniques to mitigate the inconsistency. Various baseband digital predistortion (DPD) schemes have emerged as effective approaches to mitigate the sources of distortions in the radio systems and, more precisely, the PA stage. These schemes have generally been inspired either by the Volterra series or neural networks and are used to predict or linearize the output of several types of PAs that are driven with wideband signals (envelope tracking amplifiers, Doherty PAs) [1, 2].

One of the critical issues in the practical application of these schemes, as a behavioral model or linearizer, is the availability of a systematic approach for determination of minimum dimensions of the problem, namely the minimum order of nonlinearity and memory depth needed to accurately capture the distortion exhibited by the device under test (DUT). This is particularly important, as the simple approach, which consists in over-dimensioning of the scheme by using a large nonlinearity order and memory depth, leads to unnecessary complexity.

The DPD function usually treats the PA as a "black box", without *a priori* knowledge of the physical mechanisms and circuit properties, resulting in a non-ideal response. The setting of the DPD models' parameters (memory depth, nonlinearity order) is essentially done in an *ad hoc* manner [3, 4]. Little attention has been paid to the embedding/integration of system parameters to confine Volterra series-based behavioral models in order to reduce their complexity, thus enhancing their robustness and extrapolation capability. This situation has resulted in some models of high complexity, arduous to implement, and others that have limited learning capability and robustness as the resultant model is generally not system representative. As a dynamic, nonlinear system a PA can be described by its system parameters. These parameters are to be distinguished from those used for the corresponding behavioral model. Prior knowledge of the system parameters, if used to constrain the settings of the model parameters (as represented by the dashed rectangle in Fig. 1) leads to more robust models.

In a wideband signals scenario, nonlinear dynamic distortion behavior is pronounced and the usual empirical approach to model parameters determination is limited. In this paper, a number of well-known system parameters identification methods are discussed, implemented and used to confine Volterra series modeling two power amplifiers driven with wideband signals with up to 40 MHz bandwidth. In Section II, a description of the procedure for estimating the PA

EMRG Research Group, Department of Electrical and Computer Engineering, University of Waterloo, 200 University Ave W., Waterloo, ON, Canada N2L-3G1
Corresponding author:
Slim Boumaiza
Email: sboumaiz@ecemail.uwaterloo.ca

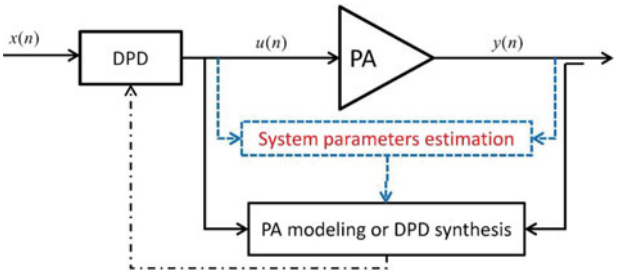

Fig. 1. System parameters-based modeling and DPD.

nonlinearity order using a complexity-reduced method is presented. In Section III, the characterization of the PA memory effects is discussed, and a suitable approach for its identification is presented. Section IV is devoted to the integration of the estimated system parameters in the Volterra series model, in order to address the problem of an excessive number of coefficients and multipliers-accumulators needed for its construction and implementation.

II. NONLINEARITY ORDER ESTIMATION

Estimating the optimal nonlinearity order, called hereafter *NL*, is a compromise between weakening the linearization capability by using an under-dimensioned model and avoidance of the over-modeling problems, i.e. the degradation of the accuracy due to an excessive conditioning number and the increase of computational complexity. For example, the practical realization of a predistorter involves a continuous online DPD and an infrequent offline identification module; therefore, simplification of the former by determining the lowest nonlinearity order at the cost of increasing the latter. Furthermore, estimation of the optimal nonlinearity order is particularly important in the assessment of linearizability (i.e. the associated complexity of the corresponding DPD) of various PAs, where the identification of the actual *NL* is crucial.

A) Nonlinearity order estimation

Estimating the *NL* of the PA should precede the estimation of the memory depth as transistor static nonlinearity dominates the distortions of the PA. Hence, a memoryless PA representation is adopted for estimation of PA nonlinearity as

$$y(n) = \sum_{i=1}^{K} a_i \cdot x(n) \cdot |x(n)|^{i-1} \tag{1}$$

where $x(n)$ is the PA input and $y(n)$ is the PA output, which is assumed to be independently and normally distributed around a polynomial trend. Per null assumption [5], the optimal nonlinear order, $NL = K_{opt}$, is defined as the one for which the least-squares estimation (LSE) solution for a higher-order problem has $a_i = 0$ for $i > NL$ [5]. The residual error variance attributed to the estimation routine generally decreases when increasing the nonlinearity order, until it reaches a given threshold. The residual error variance, σ_K^2, is defined in (2)

$$\sigma_K^2 = \frac{\varepsilon_K^2}{N - K - 1} \tag{2}$$

where ϵ_K and N denote the residual error and the number of measurement data, respectively.

$$\varepsilon_K^2 = \sum_{i=1}^{N} \left| y_i - P_K(x_i) \right|^2 \tag{3}$$

The drawback of this procedure resides in the LSEs computational complexity, which is $O(N^3)$, and the need to run it *NL* times. To alleviate this problem, the LSE problem was first reformulated, and then the Euclidean polynomials' basis was replaced with orthogonal ones.

B) Computational complexity reduction

1) LSE PROBLEM REFORMULATION

The LSE-based solution of (1) can be obtained by solving

$$X_{comp} \cdot a = Y \tag{4}$$

where X_{comp}, a and Y denote the input signal non-square matrix, the unknown coefficients' vector, and the output signal vector, respectively

$$X_{comp} = \begin{pmatrix} x(1) & x(1)|x(1)| & \dots & x(1)|x(1)|^{K-1} \\ x(2) & x(2)|x(2)| & \dots & x(2)|x(2)|^{K-1} \\ \dots & \dots & \dots & \dots \\ x(N) & x(N)|x(N)| & \dots & x(N)|x(N)|^{K-1} \end{pmatrix},$$

$$a = \begin{pmatrix} a_1 \\ \vdots \\ a_K \end{pmatrix}, \; Y = \begin{pmatrix} y(1) \\ \vdots \\ y(N) \end{pmatrix}$$

X_{comp} can be rewritten as a product of two matrices where the first one, X_d, is a complex-valued and diagonal matrix, and the second one, X_{real}, is a non-diagonal, non-squared, and real-valued Vandermonde matrix.

$$X_{comp} = X_d \cdot X_{real} \tag{5}$$

where

$$X_d = \begin{pmatrix} x(1) & 0 & \dots & 0 \\ 0 & x(2) & \dots & 0 \\ \dots & \dots & \dots & \dots \\ 0 & 0 & \dots & x(N) \end{pmatrix}$$

$$X_{real} = \begin{pmatrix} 1 & |x(1)| & \dots & |x(1)|^{K-1} \\ 1 & |x(2)| & \dots & |x(2)|^{K-1} \\ \dots & \dots & \dots & \dots \\ 1 & |x(N)| & \dots & |x(N)|^{K-1} \end{pmatrix}$$

Using (5), (4) can be rewritten as

$$X_{real} \cdot a = X_d^{-1} \cdot Y \tag{6}$$

https://doi.org/10.1017/S1759078713000056 Published online by Cambridge University Press

The reformulation of the LSE problem using (5) transformed the computationally cumbersome pseudo-inversion of the complex and ill-conditioned X_{comp} matrix to the inversion of two much simpler matrices – diagonal matrix, X_d, and real matrix, X_{real} – thereby significantly decreasing the computational complexity. This allows for a reduction of the number of operations required from $\left(\frac{11}{6}N^3+\frac{1}{2}N^2-\frac{64}{3}N\right)$ to $\left(\frac{1}{3}N^3+\frac{5}{2}N^2+\frac{1}{6}N\right)$.

2) ORTHOGONAL BASIS DESCRIPTION

The solution to the problem defined in (6) is

$$\hat{a}=(X_{real}^t\cdot X_{real})^{-1}\cdot X_{real}^t\cdot X_d^{-1}\cdot Y \tag{7}$$

where $\hat{a}$ is the estimate of a and t defines matrix transpose operator.

Since X_d is a diagonal matrix, the complexity of the computation of (7) is largely produced by the inversion of matrix $X_{real}^t\cdot X_{real}$. The complexity of the latter can be significantly alleviated if the polynomial function, $P_K(|x(n)|)$, is expressed on an orthogonal basis, ψ, instead of the popular Euclidean one as

$$P_K(|x(n)|)=\sum_{i=1}^{K}b_i\cdot\psi_{i-1}(|x(n)|) \tag{8}$$

$$X_{orth,real}=\cdot\begin{pmatrix}1 & \psi_1(|x(1)|) & \dots & \psi_{K-1}(|x(1)|)\\ 1 & \psi_1(|x(2)|) & \dots & \psi_{K-1}(|x(2)|)\\ \dots & \dots & \dots & \dots\\ 1 & \psi_1(|x(N)|) & \dots & \psi_{K-1}(|x(N)|)\end{pmatrix} \tag{9}$$

Thus, (7) can be written as

$$\hat{b}=(X_{orth,real}^t X_{orth,real})^{-1}X_{orth,real}^t X_d^{-1}Y \tag{10}$$

where $\hat{b}$ is the estimate of b, which designates the coefficients of the orthogonal polynomial. Knowing that

$$\sum_{n=1}^{N}\psi_i(|x(n)|)\psi_j(|x(n)|)=0\quad\text{for}\quad i\neq j \tag{11}$$

then $X_{orth,real}^t\cdot X_{orth,real}$ is a diagonal matrix easily inverted.

Several orthogonal polynomial definitions have been reported in the literature. The authors in [6] adopted an orthogonality definition, where the orthogonal basis is dependent on input signal statistics. Alternatively, the authors in [7] proposed a Schmidt ortho-normalization, which has a significant complexity burden. To tackle these problems, the orthogonal basis used in this work was constructed using the three-term recurrence formula [5] as

$$\psi_{i+1}(r)=r\psi_i(r)-\alpha_{i+1}\psi_i(r)-\beta_i\psi_{i-1}(r) \tag{12}$$

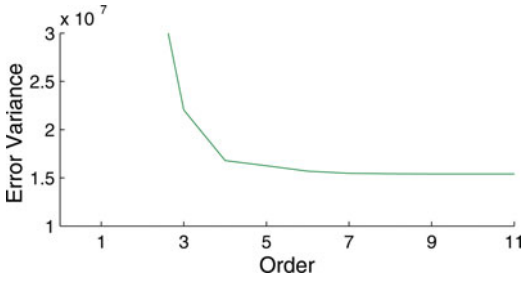

Fig. 2. Error variance applied to the PAs under test.

$$r=|x|;\ \alpha_{i+1}=\frac{\sum_{n=1}^{N}r(\psi_i(r(n)))^2}{\sum_{n=1}^{N}(\psi_i(r(n)))^2};\ \beta_i=\frac{\sum_{n=1}^{N}(\psi_i(r(n)))^2}{\sum_{n=1}^{N}(\psi_{i-1}(r(n)))^2}$$

where α_{i+1} and β_i are calculated to maintain orthogonality relation (12), and $\psi_0(r)=1$; $\psi_1(r)=r\psi_0(r)-\alpha_1\psi_0(r)$.

C) Validation

The previously proposed technique was used to estimate the corresponding *NL* of an oversampled record of the output of a high-power single-ended gallium nitride (GaN) PA, driven with a two-carrier 1001 wideband code division multiple access (WCDMA signal), which was sampled at a frequency of 122.88 MHz ($Ts=8.13$ ns). According to Fig. 2, the *NL* was estimated as equal to 7, and the error variance remained constant for a higher nonlinearity order.

III. PA MEMORY SPAN ESTIMATION

Three potential approaches can be envisaged for estimation of the memory effect span in the response of a given PA, namely physical, empirical, and systematic methods. A physical approach relies on accurate understanding and detection of the physical mechanisms behind memory effects, such as nonlinear reactance in the transistor, non-constant frequency response of biasing, and the input and output matching networks [8]. In spite of the theoretical soundness of this approach, it is too complex to implement.

Alternative methods (empirical and systematic) that exploit the measured input/output signals of the PA are usually found to be more practical. Empirical methods can be performed [3] by varying the parameters that describe the memory effect span in a given model and then retaining the values that optimize a given cost function, such as the normalized mean square error, thereby revealing the best modeling accuracy.

On the other hand, a systematic method can be used to estimate memory effects span of a PA by determining its embedding dimension. In fact, the objective of system embedding is to transform the single observed-variable-based description of a dynamic nonlinear system into a multivariate description [9]. The multivariate vector, called phase space, is made of a set of delayed versions of the observed variable, which also stand for the memory effects in a PA. The phase space is used to trace the orbit of the system in a multi-dimensional space. The determination of the system embedding parameters

https://doi.org/10.1017/S1759078713000056 Published online by Cambridge University Press

is known as phase space reconstruction [10, 11]. The systematic approach, being more reliable and less complex, is preferred over the empirical one which is known for its heavy computational requirements, sensitivity to input signal statistics, and potential convergence to local minima.

A) PA phase space reconstruction

The identification of the memory effect span in a PA's response can be turned into a problem of phase space reconstruction of a dynamic nonlinear system. The set formed by the current sample of the output signal's envelope, $y(n)$ (which represents the system observation variable), and its delayed samples, $y(n-m)$, $\ldots$, $y(n-(d-1)\cdot m)$, capture the memory effect

$$\left[y(n), y(n-m),\ldots, y(n-(d-1)\cdot m)\right], \text{ where } d \geq 1 \quad (13)$$

where m, referred to hereafter as the memory index, designates the time index separating two consecutive components in phase space and can be expressed as a function of the sampling period (T_s) as $m = \frac{\tau}{Ts}$, where τ is the memory lag. m is chosen such that components of the reconstructed vector in (13) ensure maximum independency. The number of components in phase space required to describe dynamic nonlinear system response is represented by d and is usually called minimum embedding space dimension and commonly designated as memory depth. Hence, the memory span (S) of the dynamic nonlinear system is defined as $S = (d-1)\times\tau = (d-1)\times m \times Ts$ (s). The determination of the value of m has to precede the estimation of the embedding dimension (d).

B) Memory index estimation

The estimation of the value of m is performed using the mutual information (MI)-based approach [10, 11], since it is preferred to an autocorrelation function when dealing with dynamic nonlinear systems. Mutual information, $MI(m)$, is defined in (14), where P_1 is the probability density of the data sample, and P_2 is the joint probability of a given sample and the delayed samples. The proper value of m corresponds to the first minimum value of MI, indicating minimum dependence.

$$\begin{aligned} MI(m) = &\sum_{y_n}\sum_{y_{n-m}} p_2(y_n, y_{n-m}) \log_2\left(p_2(y_n, y_{n-m})\right) \\ &- \sum_{y_n} p_1(y_n) \log_2\left(p_1(y_n)\right) \\ &- \sum_{y_{n-m}} p_1(y_{n-m}) \log_2\left(p_1(y_{n-m})\right) \end{aligned} \quad (14)$$

The proposed procedure was applied to the above-mentioned PA; and, as per Fig. 3, the MI reached its first minimum at approximately $m = 3$

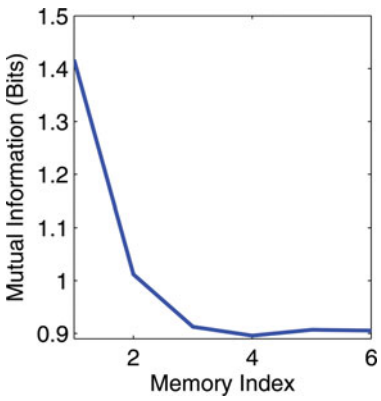

Fig. 3. Mutual information-based system time index estimation.

C) Embedding dimension estimation

The minimum embedding parameter (d) and, consequently, the memory depth of a dynamic nonlinear system can be estimated using singular value decomposition (SVD) or false nearest neighbors (FNN)-based methods [12]. The SVD-based approach is, to some extent, subjective, as the number of large singular values may depend on the DUT to be modeled and the accuracy and statistics of the data, as they are dependent on the dynamics of the system itself.

The FNN method increases the dimension of the embedding until a preset criterion is met. The FNN method was initially used to determine the set of independent variables, the terminations voltages, and their derivatives, needed to accurately predict the currents at RF circuit's terminations [11]. A first attempt of the application of the FNN method to find a systematic determination of the memory effect depth of a PA was given in [10] (where the definitions of the phase space and convergence criteria are given in [12]), but was applied only to the input signal of the PA.

In this paper, the FNN method defined in [13] is applied to the envelope of the PA output to capture the memory effects, thereby leading to a better assessment of the embedding dimension. The FNN method estimates the embedding parameter iteratively by increasing parameter d and thus the phase space dimension, while checking if the correct space (reconstruction phase space) is reached. In fact, the theory claims that, in a lower than required embedding dimension, the neighborhood relation between different points in that space is false and is true only if the embedding dimension is reached.

To check the neighborhood relation in a phase space with d dimension for only one sample (indexed here by n) in the dataset, define $v(n) = \left[y(n), y(n-m),\ldots, y(n-(d-1)\cdot m)\right]$ and $v(n') = \left[y(n'), y(n'-m),\ldots, y(n'-(d-1)m)\right]$, where n' is a given index to be estimated such that $v(n')$ is the nearest neighbor to $R_d(n,m) = |v(n) - v(m)|$ as the Euclidean distance between two points, where $m \in [1\,..\,L]$ and L is the dataset size, n'' is the index in the dataset that minimizes $R_d(n,m)$ as

$$R_d(n, n') = \min_{m\in[1..L]} (R_d(n, m)) \quad (15)$$

The theory defines Q, expressed in (16), as the next phase space added distance

$$Q(n) = \frac{\left|y(n' - d\cdot m) - y(n - d\cdot m)\right|}{R_d(n, n')} \quad (16)$$

https://doi.org/10.1017/S1759078713000056 Published online by Cambridge University Press

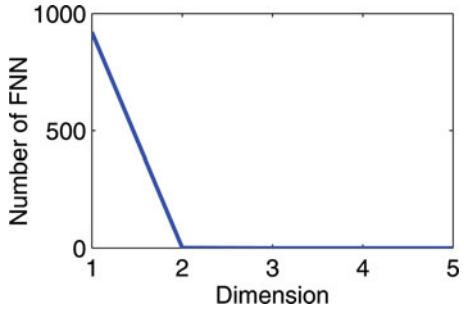

Fig. 4. FNN-based system memory depth estimation.

When Q is smaller than a given threshold, which has been recommended to be equal to 15 in [13], $v(n')$ is considered as a true neighbor to point $v(n)$; otherwise, it is said to be a false neighbor.

For a given dimension, d, it is sufficient to check the neighborhood relation for an arbitrary number of samples in the dataset, i.e. $n \in [1 \,..\, L']$ where $L' << L$. The number of false neighbors is counted in the phase space defined by d dimension. Dimension d continues increasing, and the correct phase space is said to be identified when the number of false neighbors is reduced to zero. Figure 4 shows the result of neighborhood relation tracking of 1000 samples when d is increasing for the already mentioned PA. The number of FNN relations reaches zero, starting from an embedding dimension equal to $d = 2$, revealing that the reconstruction phase space should be formed by two components $[y(n), y(n-3)]$.

IV. EMBEDDING DIMENSION-BASED VOLTERRA SERIES MODEL

A) Formulation

The Volterra series, being a general framework to model nonlinear dynamic systems, represents a very suitable candidate to model and linearize PAs. Considered as computationally heavy, several transformations, such as envelope extraction, discretization, and truncation, are usually applied to transform the Volterra series into a low-pass equivalent (LPE) Volterra series, as per (17)

$$y(n) = \sum_{\substack{p=1 \\ p=p+2}}^{NL} \sum_{i_1}^{M} \cdots \sum_{i_p}^{M} h_p(i_1,\ldots,i_p) \prod_{j=1}^{(p+1)/2} x(n-i_j) \cdot \prod_{j=(p+3)/2}^{p} x^*(n-i_j) \quad (17)$$

where $x(n)$ and $y(n)$ designate the input and output envelopes, NL is the nonlinearity order, M is the memory depth, and h_p are the baseband equivalent Volterra kernels. In (17), only the odd-powered terms are retained; and, redundant terms, due to kernel symmetry, are excluded.

Lacking practical methods to determine the nonlinearity order and memory depth of LPE Volterra series, empirical approaches are usually followed. These approaches consist of increasing the model parameters values (NL, M) until an acceptable model is obtained, at the cost of exponentially increasing the number of coefficients of the LPE Volterra series, thereby yielding a computationally heavy model.

To overcome this issue, many simplification attempts have been proposed in the literature. One such attempt involves removing cross terms in the LPE Volterra series, thereby obtaining the memory polynomial (MP) model, a one-dimensional approximation of nonlinear finite impulse response systems [1]. Dynamic deviation reduction [14] is another LPE Volterra series simplification approach and is aimed at reducing complexity by introducing a third parameter to control model dynamics that is yet to be determined empirically.

Integrating the estimated system parameters determined according to the procedure described earlier in an LPE model would avoid the use of these empirical approaches and, thus, mitigate the burden associated with the excessive number of coefficients without loss of generality. The replacement of memory effects parameter, M, in (17) with the embedding dimension, d, and the memory index, m, leads to the optimized Volterra series given in (18), where

$$y(n) = \sum_{\substack{p=1 \\ p=p+2}}^{NL} \sum_{i_1}^{d-1} \cdots \sum_{i_p}^{d-1} h_p(i_1,\ldots,i_p) \prod_{j=1}^{(p+1)/2} x(n-m\cdot i_j) \cdot \prod_{j=(p+3)/2}^{p} x^*(n-m\cdot i_j) \quad (18)$$

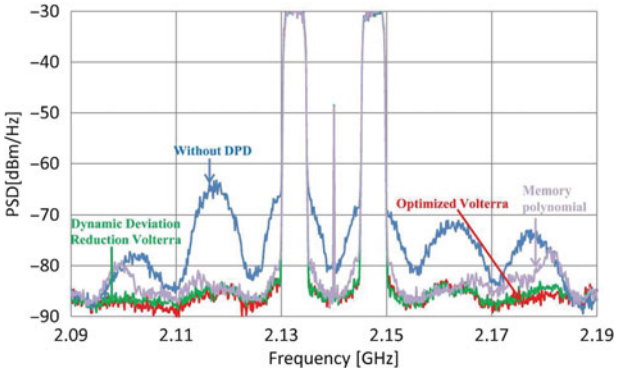

Fig. 5. Optimized Volterra vs. memory polynomial vs. dynamic deviation reduction Volterra DPDs' linearization results of a 45 W class AB GaN PA driven with 20 MHz (2C 1001) WCDMA signal.

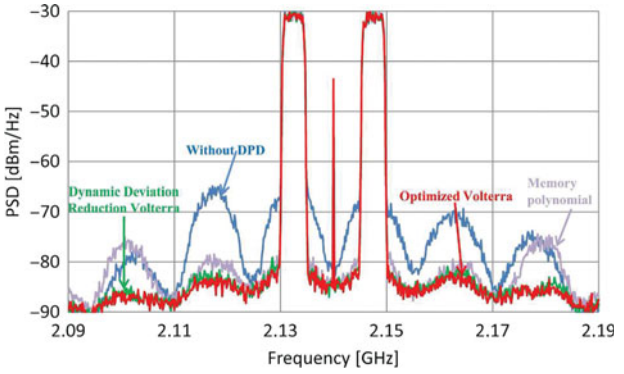

Fig. 6. Optimized Volterra vs. memory polynomial vs. dynamic deviation reduction Volterra DPDs' linearization results of a 200 W Doherty PA driven with 20 MHz (2C 1001) WCDMA signal.

https://doi.org/10.1017/S1759078713000056 Published online by Cambridge University Press

Table 1. Optimized Volterra, DDR Volterra and memory polynomial models' parameters and linearization performance of the 20 MHz WCDMA signal test case.

PA	Model	Parameters	Number of coefficients	ACLR Offset at IMD3	Offset at IMD5
	Without DPD			−35	−43
Class AB GaN PA	Memory polynomial	$NL = 7, M = 5$	20	−52	−47
	DDR Volterra	$NL = 7, M = 3, r = 2$	91	−53	−54
	Optimized Volterra	$NL = 7, m = 3, d = 2$	40	−53	−54
	Without DPD			−36	−45
Doherty LDMOS PA	Memory polynomial	$NL = 7, M = 9$	36	−49.5	−45
	DDR Volterra	$NL = 7, M = 3, r = 2$	91	−52	−55
	Optimized Volterra	$NL = 7, m = 3, d = 2$	40	−52	−55

Table 2. Optimized Volterra, DDR Volterra, and memory polynomial models' parameters and linearization performance of the 40 MHz LTE signal test case.

PA	Model	Parameters	Number of coefficients	ACLR Near carrier	Offset at IMD3
	Without DPD			−33	−33
Class AB GaN PA	DDR Volterra	$NL = 7, M = 6, r = 2$	277	−44	−45
	Optimized Volterra	$NL = 7, m = 2, d = 3$	231	−48	−49
	Without DPD			−33	−34
Doherty LDMOS PA	DDR Volterra	$NL = 7, M = 6, r = 2$	277	−43	−44
	Optimized Volterra	$NL = 7, m = 2, d = 3$	231	−48	−49

To assess the proposed model linearization performance and robustness to transistor technology, PA topology, and signal characteristics variations, several measurements were considered. Several models are used to linearize two different PAs when driven with a 20 MHz WCDMA signal, as in Section IV(B), and driven by a 40 MHz long-term evolution (LTE) signal as in Section IV(C).

B) 20 MHz WCDMA signal test case

In this experimentation, the driving signal is a 2C (1001) WCDMA signal with 20 MHz bandwidth. Two different DUTs are considered here, a 45 W class AB GaN PA and a 200 W laterally diffused metal oxide semiconductor (LDMOS) Doherty PA. To assess the optimized Volterra modeling and predistortion performance, its linearization performance is compared with several PA behavioral models, namely the MP model and the Dynamic Deviation Reduction (DDR) Volterra model. Based on the previous analysis, the memory index, m, the embedding dimension, d, and the nonlinearity order, NL, of the optimized Volterra series are estimated systematically. For the remaining models, parameters were estimated empirically targeting best possible results. Table 1 summarizes the chosen parameters values and the resultant models' complexity in terms of number of coefficients. The corresponding linearization results are shown in Figs 5 and 6, respectively, and the adjacent channel leakage power ratio (ACLR) performances are gathered in Table 1.

It is shown that for the two considered DUTs, both the optimized Volterra series DPD and DDR Volterra DPD showed excellent linearization capability and outperformed the MP model with up to 10 dB better linearization performance (−55 dBc versus −45 dBc around IMD5 in the Doherty PA case). In terms of complexity, the optimized Volterra used slightly more coefficients than the MP DPD (40 vs. 36). However, the proposed model required a significantly lower number of coefficients when compared with DDR Volterra (40 vs. 91).

C) 40 MHz LTE signal test case

In this experimentation, the driving signal is a 40 MHz multicarrier LTE signal composed of a 15 MHz LTE signal and a 10 MHz LTE signal with a 15 MHz guard band. The two previously mentioned PAs are also considered in this experiment (45 W class AB GaN PA and a 200 W LDMOS Doherty PA). To assess the optimized Volterra modeling capability, its linearization performance is compared to the DDR Volterra model. However, in this scenario, the MP model is discarded due to its poor linearization performance in wideband scenarios. Based on the previous analysis, the memory index, m, the embedding dimension, d, and the nonlinearity order, NL, of the optimized Volterra series are estimated

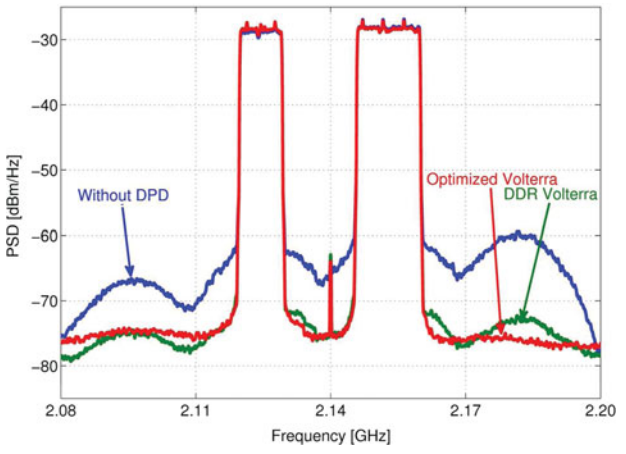

Fig. 7. Optimized Volterra vs. dynamic deviation reduction Volterra DPD's linearization results of a 45 W class AB GaN PA driven with 40 MHz LTE signal.

https://doi.org/10.1017/S1759078713000056 Published online by Cambridge University Press

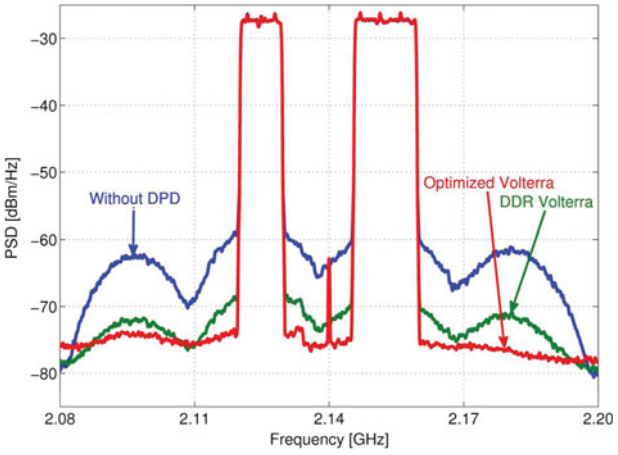

Fig. 8. Optimized Volterra vs. dynamic deviation reduction Volterra DPDs' linearization results of a 200 W Doherty PA driven with 40 MHz LTE signal.

systematically. For the remaining models, parameters were estimated empirically targeting best possible results. Table 2 summarizes the chosen parameters values and the resultant models complexity in terms of number of coefficients. The corresponding linearization results are shown in Figs 7 and 8, respectively, and the ACLR performances are gathered in Table 2.

It is shown that for the two considered DUTs, the optimized Volterra model outperformed the DDR Volterra model in terms of linearization performance and complexity. In fact, the proposed model allows for 4–5 dB better linearization performance (−48 dBc vs. −43 dBc in the Doherty PA case) with 20% lower number of coefficients (231 vs. 277).

V. CONCLUSION

A systematic determination of a PA's system parameters, namely the nonlinearity order, memory index, and the embedding dimension, is possible. The integration of these parameters into the LPE Volterra series significantly reduced its complexity burden and overcame the limitations of empirical investigation. Through a multitude of linearization measurements, the optimized Volterra series' robustness to PA design and signal variations was successfully proven. The determination of the embedding dimension is particularly important to the development of DPD schemes needed to linearize PAs driven with extended bandwidths and multi-carriers signals, as these involve strong memory effects and consequently a large number of coefficients and multipliers-accumulates.

ACKNOWLEDGEMENT

The authors would like to acknowledge the financial support of Ericsson Canada, the Ontario Research Fund (ORF), the Canada Foundation for Innovation (CFI), and the Natural Sciences and Engineering Research Council (NSERC) of Canada. The authors would like also to thank Freescale Semiconductor, Inc., Tempe, AZ, for providing the device under test.

REFERENCES

[1] Pedro, J.C.; Maas, S.A.: A comparative overview of microwave and wireless power-amplifier behavioral modeling approaches. IEEE Trans. Microw. Theory Tech., **53** (2005), 1150–1163.

[2] Isaksson, M.; Wissel, D.; Rönnow, D.: A comparative analysis of behavioral models for rf power amplifiers. IEEE Trans. Microw. Theory Tech., **54** (1) (2006), 348–359.

[3] Ku, H.; Kenny, S.: Behavioral modeling of nonlinear RF power amplifiers considering memory effects. IEEE Trans. Microw. Theory Tech., **51** (12) (2003), 2495–2504.

[4] Mkadem, F.; Boumaiza, S.: Physically inspired neural network model for RF power amplifier behavioral modeling and digital predistortion. IEEE Trans. Microw. Theory Tech., **59** (4) (2011), 913–923.

[5] Forsythe, G.E.: Generation and use of orthogonal polynomials for data-fitting with a digital computer. J. Soc. Ind. Appl. Math., **5** (1957), 74–88.

[6] Raich, R.; Zhu, G.T.: Orthogonal polynomials complex gaussian process. IEEE Trans. Signal Process., **52** (2004), 2788–2797.

[7] Ohmori, S.; Guangsheng, X.; Muta, O.; Akaiwa, Y.: An adaptive predistortion method based on orthogonal polynomial expansion for nonlinear distortion compensation. The 18th Annual IEEE Int. Symp. on Personal, Indoor and Mobile Radio Communications. PIMRC '07, September 2007.

[8] Cunha, T.R.; Pedro, J.C.; Lima, E.G.: Low-pass equivalent feedback topology for power amplifier modeling, 2008 IEEE MTT-S Int. Microwave Symp. Digest, pp. 1445–1448, June 2008.

[9] Casdagli, M.: A dynamical systems approach to modeling input–output systems. Nonlinear Modeling and Forecasting, SFI Studies in the Sciences of Complexity, Proc., 1992, Vol. XII.

[10] Wood, J.; Lefevre, M.; Runton, D.; Nanan, J.-C.; Noori, B.H.; Aaen, P.H.: Envelope-domain time series (ET) behavioral model of a doherty RF power amplifier for system design. IEEE Trans. Microw. Theory Tech., **54** (2006), 3163–3172.

[11] Schreurs, D.; Wood, J.; Tufillaro, N.; Usikov, D.; Barford, L.; Root, D.E.: Construction of behavioral models for microwave devices from time domain large-signal measurements to speed up high-level design simulation, Int. J. RF Microw. Comput.-Aided Eng., **13** (2003), 54–61.

[12] Cao, L.; Mees, A.; Judd, K.; Froyland, G.: Determining the minimum embedding dimension of input–output time series data. Int. J. Bifurcation Chaos, **8** (3) (1998), 1490–1504.

[13] Abarbanel, H.D.I.: Analysis of Observed Chaotic Data, *Springer*, New York, 1996.

[14] Zhu, A.; Pedro, J.C.; Brazil, T.J.: Dynamic deviation reduction-based volterra behavioral modeling of RF power amplifiers. IEEE Trans. Microw. Theory Tech., **54** (12) (2006), 4323–4332.

Bilel Fehri (S'11) was born in Sfax, Tunisia, in 1985. He received the B.E. and M.E. degrees from Ecole Polytechnique de Tunisie, El Marsa, Tunisia, in 2009 and 2010, respectively.

In 2011, he joined the Emerging Radio Systems Group, University of Waterloo, ON, Canada, as a Research Associate and is currently working toward a Ph.D. degree in the same group. His current research interests include nonlinear dynamic systems modeling and identification applied to digital predistortion of radio frequency power amplifiers.

https://doi.org/10.1017/S1759078713000056 Published online by Cambridge University Press

Slim Boumaiza (S'00–M'04–SM'07) received the B.E. degree in Electrical Engineering from École Nationale d'Ingénieurs de Tunis, Tunis, Tunisia, in 1997, and the M.S. and Ph.D. degrees from École Polytechnique de Montréal, Montréal, QC, Canada, in 1999 and 2004, respectively.

He is currently an Associate Professor with the Department of Electrical and Computer Engineering, University of Waterloo, Waterloo, ON, Canada, where he leads the Emerging Radio System Research Group that conducts multidisciplinary research activities in the general areas of design of RF/microwave and millimeter components and systems for wireless communications. His specific current research interests include RF/digital signal processing (DSP) mixed design of intelligent RF transmitters; design, characterization, modeling and linearization of high-efficiency RF power amplifiers; and reconfigurable and software-defined transceivers.

https://doi.org/10.1017/S1759078713000056 Published online by Cambridge University Press